Results in Physics 10 (2018) 233–240

Contents lists available at ScienceDirect

Results in Physics

journal homepage: www.elsevier.com/locate/rinp

Fatigue crack propagation characteristics of rubbery materials under variable amplitude loading

Xiao-Li Wang[a,*], Mei-Ying Liao[b], You Xu[a], Xiao-Ang Liu[c]

[a] School of Automobile and Transportation Engineering, Guangdong Polytechnic Normal University, Guangzhou 510665, China
[b] Guangzhou Automobile Group Co., Ltd., Automotive Engineering Institute, Guangzhou 510640, China
[c] School of Mechanical Engineering, Hebei University of Technology, Tianjin 300130, China

ARTICLE INFO

Keywords:
Rubber
Fatigue crack
Propagation rate
Modeling
Experiment

ABSTRACT

Fatigue failure is a critical issue frequently encountered by the rubber components in service. In this work fatigue crack propagation experiments with an edge-notched pure shear specimen under variable amplitude loading, which brings effectiveness in experiment time, are carried out. Based on the dispersed data of measured crack lengths versus number of cycles, an alternative method for dealing with the dispersed data is proposed and compared with two conventional methods used in constant amplitude loading. The comparisons of the three types of methods shows that the secant method and the incremental polynomial method are not applicable whereas the proposed method with one power function is superior to characterize the crack propagation characteristics of rubbery materials. The crack propagation rate (crack propagation length per cycle) is then calculated from the determined power function, and a fatigue life prediction model for filled natural rubbery materials is established as well as applied to calculate the fatigue life of dumbbell specimens under uniaxial tension fluctuating loading. The consistence between the calculated fatigue lives and the measured lives of the dumbbell specimens validates the proposed data processing method for dealing with the dispersed measured data of crack length versus number of cycles.

Introduction

Rubbery materials have the advantage of withstanding very large strains but without permanent deformation or fracture, which make it ideal for many applications such as tires, vibration isolators, accessory drive belts and so on [1,2]. Rubber components are usually subjected to large static and fluctuating loads, and often fail due to the nucleation and propagation of defects or cracks. To prevent such mechanical fatigue failure, it is of prime importance to understand the deformation mechanisms involved during cyclic loading, and to study the fatigue crack propagation characteristics of rubbery materials.

The mechanical fatigue of rubbery materials is defined as the phenomenon that the mechanical properties of the material are gradually deteriorated due to the nucleation and propagation of the crack under dynamic loading. Some researchers found that fatigue failure of rubbery materials is due to the gradual propagation of small cracks in the rough materials under external cyclic loading [3,4], which necessitates investigations on the fatigue crack propagation characteristics of rubbery materials. Rubbery materials' crack propagation characteristic experiments were frequently conducted under constant amplitude loading [5–7], which concludes limited levels of loading and costs long experiment time. The variable amplitude loading are thus chosen to more effectively get the crack propagation measurements of the studied rubbery materials.

Establishing the mathematical model of crack propagation characteristics of rubbery materials based on the experimental data is a challenge task that is quite distinct from metal-like materials. For metal materials, Jia et al. [8] and Meng et al. [9] studied different data processing methods for determining crack propagation rate based on the directly measured crack length versus number of cycles, including seven incremental polynomial method [10], Smith method [8] and the integral method [9] derived from Paris formula [11]. However, rubbery materials' crack propagation data shows immense dispersion, especially under variable amplitude loading.

In this paper, taking an edge-notched pure shear specimen of filled natural rubbery materials used for automotive engine mounts as a studying example, a fatigue crack propagation experiment under variable amplitude loading is carried out. An alternative method of dealing with the dispersed data of the measured crack length versus number of cycles is proposed based on measured crack propagation characteristics

* Corresponding author.
E-mail addresses: xlwang55@163.com, mexlwang@scut.edu.cn (X.-L. Wang).

https://doi.org/10.1016/j.rinp.2018.05.043
Received 9 April 2018; Received in revised form 25 May 2018; Accepted 26 May 2018
Available online 31 May 2018

and the basic principle of the power law of the crack propagation rate (crack propagation length per cycle) and tearing energy of rubbery materials. The calculation results show that the crack propagation rate calculated by this method can obey the power law well. Finally, the established crack propagation rate model is applied to calculate the fatigue life of dumbbell specimens under uniaxial tension fluctuating loading. The comparison of the calculated fatigue lives and the measured lives of the dumbbell specimens shows that the crack propagation rate model based on the proposed method is appropriate in dealing with the dispersed measured data of crack length versus number of cycles.

Tearing energy and fatigue crack propagation law

Griffth [12] was the first to propose an energy based criterion to describe the fracture of brittle materials. In this approach, the energy release rate (noted G) is assumed to govern the crack initiation in a linear elastic material. Thomas [13] then extended the Griffith (1920) criterion to the tearing of rubbers [9]. They found that the amount of potential energy decrease per unit crack area, which is called the tearing energy noted T (equal to the energy release rate G), have the following equation [3]:

$$T = -\frac{\partial U}{\partial A} \tag{1}$$

where the minus means that the potential energy U decreases with increasing crack area A.

The crack propagation rate $\mathrm{d}a/\mathrm{d}N$ is used to characterize the crack propagation speed per load cycle. The fatigue crack propagation performance under the fully relaxing cycles (e.g. the minimum tearing energy equals to zero) is very important for materials. Under the fully relaxing cycles, the fatigue crack propagation behavior of rubbery materials frequently experiences four regimes [3] as shown in Fig. 1. The rupture occurs when the tearing energy T reaches or overcomes a critical value noted as T_c (Regime IV), which suggests that T_c is a material property of fracture resistance. There is also a threshold tearing energy, denoted by T_0, which means the lower limit that the mechanical crack propagation occurs. It is suggested that no mechanical crack propagation exists if $T < T_0$ (Regime I), which is also a material property of fatigue resistance. However, if there is ozone in the lab, the crack propagation proceeds at a constant rate r (much slower than the mechanical crack propagation) which attributes to ozone chemical attack when the maximum tearing energy remains below T_0. The fatigue crack propagation behavior between T_0 and T_c is divided into two regimes (Regimes II and III). The transition value of tearing energy between Regimes II and III is noted by T_t. In practice, the fatigue crack propagation in Regime III can approximately represent those in other three regimes [14,15]. Therefore, Regime III is frequently utilized to analyze the fatigue crack propagation characteristics of rubber components [14,15].

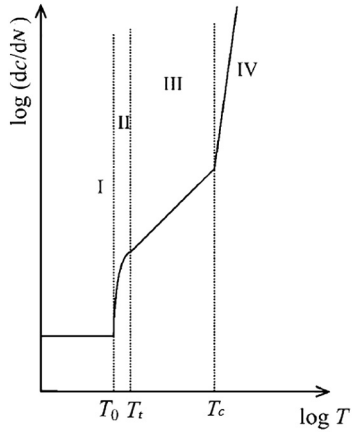

Fig. 1. Four regimes of fatigue crack propagation characteristics in rubbery materials.

The fatigue crack propagation behavior in Regime III is expressed using the following power law expression [14]:

$$\mathrm{d}a/\mathrm{d}N = AT_{\max}^{F} \qquad T_t \leqslant T_{\max} < T_c \tag{2}$$

where a is crack length, N is number of load cycles, A and F are material parameters determined from the fatigue crack propagation experiment.

The equation above can also be rewritten as:

$$\frac{\mathrm{d}a}{\mathrm{d}N} = r_c\left(\frac{T_{\max}}{T_c}\right)^{F} \tag{3}$$

where $r_c = AT_c^F$ is defined as the critical crack propagation rate corresponding to the critical tearing energy T_c. The two parameters, r_c and T_c, are determined by the material itself, which means that they are identical for one type of material [16].

It can be found from Eq. (3) that the crack propagation rate $\mathrm{d}a/\mathrm{d}N$ keeps constant under constant amplitude fluctuating loading with the minimum tearing energy equal to zero ($T_{\max}$ keeps constant), which indicates that the relation between the crack propagation length and number of cycles is linear. However, under variable amplitude loading, the crack propagation rate $\mathrm{d}a/\mathrm{d}N$ is no longer constant and the relation between the crack propagation length and number of cycles is to be investigated carefully.

Fatigue crack propagation experiment

Specimen

The pure shear specimen shown in Fig. 2 is used in the experiment since the tearing energy (T) is independent of crack size. The tearing energy can be obtained as the product of the strain energy density (W) far away from the crack tip and the specimen gauge length (h_0) [3]:

$$T = Wh_0 \tag{4}$$

The pure shear specimen (Fig. 2) has a width of 140 mm, a height of 10 mm, and a thickness of 2 mm. The specimen size in the experiment has a slightly deviation from the nominal size since the inevitable error during the manufacturing process. The largest deviation from the nominal size is within 0.3 mm, 0.72 mm and 0.03 mm in width, height and thickness, respectively. The vulcanization temperature is up to 150 °C and the curing time is 10 min.

The specimen geometry should meet the appropriate ratio of width to height in order to assure that the specimen effective area is under pure shear state [4]. In general, the ratio of width to height (l/h_0) with no smaller than 5 is preferred; the specimen is supposed to be thin enough to reduce the temperature accumulation effect on fatigue characteristics. In the meanwhile, the width area between 1.5 and 2 times height from the free end couldn't be used for measuring fatigue crack propagation characteristics due to boundary effect. Therefore, in the experiment, the pure shear specimen has an initial crack length of 25 mm, which is greater than $2h_0$.

The crack orientation should be perpendicular to the tensional

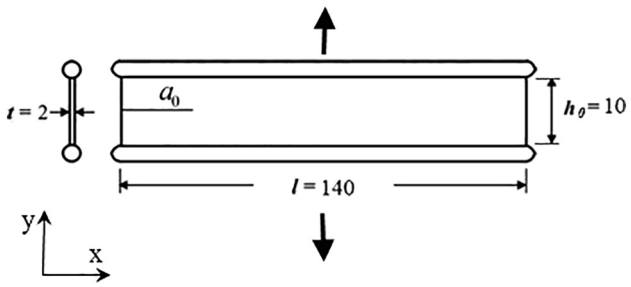

Fig. 2. The pure shear specimen.

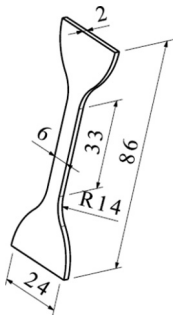

Fig. 3. The configuration of the dumbbell specimen.

loading direction as well as within the middle plane of the specimen when given the initial crack. It is noted that the measurement must be stopped and a new crack must be given again if the crack propagation direction changes or bifurcates in the experiment. When the crack grows and arrives at the area that is $2h_0$ length from the other free end, one new specimen should be taken place of the old one.

Another specimen with a dumbbell-like configuration (in Fig. 3) is made to validate the established fatigue crack propagation model. The dumbbell specimen was designed in accordance with the ASTM standard (ASTM: D4482-11) [17].

The material strength parameters

The material's tensile properties are needed to be determined firstly before the rubber crack propagation experiment and the conventional fatigue experiment. The tensile properties (such as tensile strength) are helpful to determine the upper limit of load imposed on the specimen during the fatigue experiments. The quasi-static stretching tests with the two types of specimens shown in Figs. 2 and 3 are thus carried out in the Instron electronic universal testing machine. The laboratory temperature is about 23 ˚C, and the strain rate of the stretching process is 0.01per second.

The engineering strain and stress data in the gauge length are recorded during the tests, which are used to determine the critical load such as the tensile strain at break, ultimate tensile strength and the critical tearing energy. The recorded strain is measured using the laser extensometer, and the recorded stress is calculated using the load measured from the force sensor divided by the initial sectional area of the specimen.

The test process with dumbbell specimen is shown in Fig. 4. The tensile strain at break, ultimate tensile strength and the 300% elongation modulus of the dumbbell specimen are shown in Table 1. In the following fatigue tests with the dumbbell specimens, the tensile strain in Table 1 is the upper limit of load imposed on the specimen.

Meanwhile, the quasi-static stretching test with the pure shear specimen is carried out to determine the maximum load applied to the pure shear specimen during the fatigue crack propagation experiments. In the experiment, three identical pure shear specimens (noted by s1–s3) are repeated. The measured engineering stress and engineering strain curve is shown in Fig. 5. The gauge height h0 for measuring the three specimens' strain using laser extensometer has the value of 8.59 mm, 10.61 mm and 10.11 mm, respectively.

The engineering stresses (σ) and engineering strain (ε), as recorded in Fig. 5, are substituted into the following Eq. (5) to solve the critical strain energy density (W_b) at break of the rubbery materials.

$$W_b = \int_0^{\varepsilon_b} \sigma d\varepsilon \tag{5}$$

The critical tearing energy (T_c) at break can be obtained using Eq. (4) and the determined critical strain energy density (W_b) from Eq. (5). The calculation results of the strain energy density (W_b) and the critical tearing energy (T_c) of the three pure shear specimens are shown in Table 2. The median [17] of the three specimens' critical tearing energy is taken as the critical tearing energy of the tested rubbery materials, which has a value of 17.4007 kJ/m^2. The corresponding tensile strain at

Fig. 4. The process of measuring strain with one laser extensometer.

Table 1
Mechanical properties of the studied rubbery materials.

Temperature (°C)	Density (g/cm^3)	Shore hardness	Tensile strain at fracture (%)	Ultimate tensile strength (MPa)	300% elongation modulus (MPa)
23	1.05	48	620	26	4.4

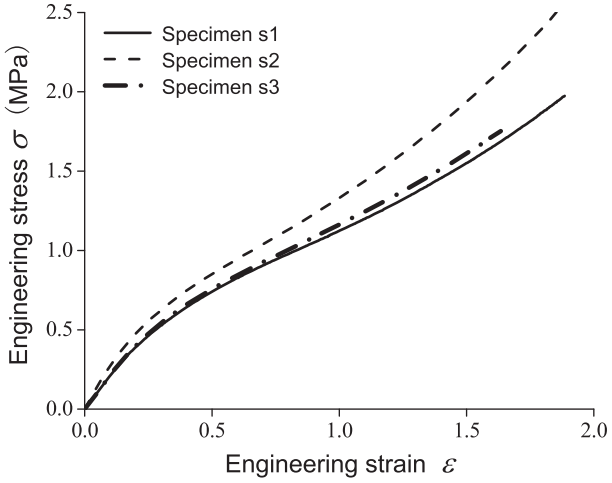

Fig. 5. The engineering stress versus engineering strain.

Table 2
Mechanical parameters of the studied rubbery materials at break in tension.

Specimens	Engineering stress σ_b (MPa)	Engineering strain ε_b (%)	Strain energy density W_b (MPa)	Tearing energy T_c (kJ/m^2)
s1	1.9740	188.54	2.0241	17.4007
s2	2.7606	199.44	2.7604	29.2880
s3	1.7535	163.49	1.6184	16.3669

break is 188.54%. Therefore, during the fatigue crack propagation test with the pure shear specimen, the strain applied on the specimen should be less than 188.54%, and the maximum tearing energy should be less than 17.4007 kJ/m^2.

Fatigue crack propagation experiment

Experimental method

The fatigue load of rubbery materials is much less than the maximum static load that the material could withstand. Therefore, the tearing energy of the edge-notched pure shear specimens during crack propagation tests is far less than the critical tear energy T_c of the rubbery materials. Fatigue tests were conducted on a displacement-controlled machine. The measured strain and stress can be used to calculate the corresponding tearing energy, which is frequently used as the governing variable of fatigue crack propagation.

The crack propagation tests in this work were carried out under the load of $R = 0$ where R is defined as the ratio of the minimum tearing energy and the maximum tearing energy during one cycle. The crack propagation tests of rubbery materials are mainly to obtain the crack propagation characteristics of the materials, namely the relationship between the crack propagation rate of rubbery materials and the maximum tearing energy noted as T_{max}. In order to quickly obtain the crack propagation test data of rubbery materials at $R = 0$, variable amplitude loading is forced on the specimens.

Fatigue tests were conducted at room temperature and at atmospheric pressure in open air. The waveform of the fatigue cycle was sinusoidal with variable amplitude. Before testing, initial cracks of various lengths were cut into the edge of the rubber specimens with a very sharp razor blade.

Two groups of edge-notched pure shear specimens were required to be produced in the experiment. The first one was used to determine the tearing energy T of the cyclic loading by integrating the unloading stress versus strain curve in the gauge length and combing with Eq. (4); the second was used to determine the rate of crack propagation rate da/dN by measuring the crack length a and recoding the corresponding number of cycles N. It should be noted that the loads imposed on the two groups of specimens are identical. Based on the measurements of the two sets of specimens, the measured curve between the crack propagation rate and the tearing energy can be obtained. Three repeated experiments were carried out using three edge-notched pure shear specimens (s4–s6) for determining the crack propagation rate of the rubbery materials.

The crack propagation tests with the pure shear specimen were carried out on one servo hydraulic machine, as shown in Fig. 6. The CCD camera is used to photograph the crack and output the crack length a in real time through the data processing system with the CCD.

The analysis and measured data of crack propagation

In the crack propagation tests of rubbery materials, the imposed

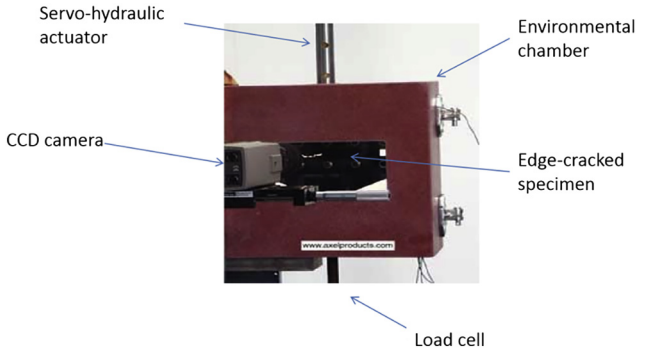

Fig. 6. The hardware system for fatigue crack propagation experiments [17].

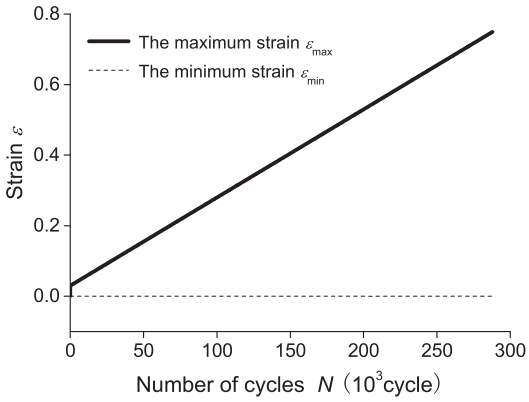

Fig. 7. The imposed variable amplitude loading in the strain-controlled experiments.

strain load are shown in Fig. 7. It can be found that the minimum strain remains zero and the maximum strain is linearly increased with the number of cycles. The maximum strain has been increased to 75%, which is about 40% of the tensile strain of the specimen at break. The corresponding maximum tearing energy is shown in Fig. 8, and the value of the minimum tearing energy remains zero.

The crack propagation length $\Delta a = a - a_0$, where a and a_0 represent the current crack length and the initial crack length on the specimen, respectively. The initial crack length a_0 was prefabricated before experiment. The number of cycles N and the corresponding crack propagation length a were measured, as shown in Fig. 9.

As shown in Figs. 7 and 9, the crack grows faster with the increase of the maximum strain (the slope of the curve in Fig. 9 is getting steeper with the number of cycles). It can be found from Figs. 7 and 8 that the maximum tearing energy increases with identical slope of the maximum strain, but remains stable and even decreases between the number of cycles about 200,000 and 250,000. However, the crack propagation rate keeps increasing at the numbers of cycles larger than 200,000. The reason for this phenomena is mainly due to the stress softening effect and permanent deformation of the rubbery materials.

In order to obtain the relationship between the crack propagation rate and the tearing energy of the rubbery materials, the key is to determine the crack propagation rate with the measured crack length data. It can be seen from Fig. 9a that the crack length increases gradually with the number of cycles globally. However, due to the factors such as the light, the measured crack length data can fluctuate locally (shown in Fig. 9b), which leads to various attempt of data processing method for modeling the crack propagation behavior.

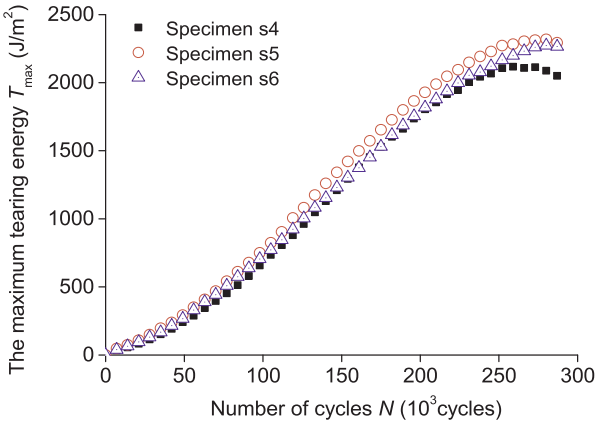

Fig. 8. The relationship between the maximum tearing energy versus number of cycles.

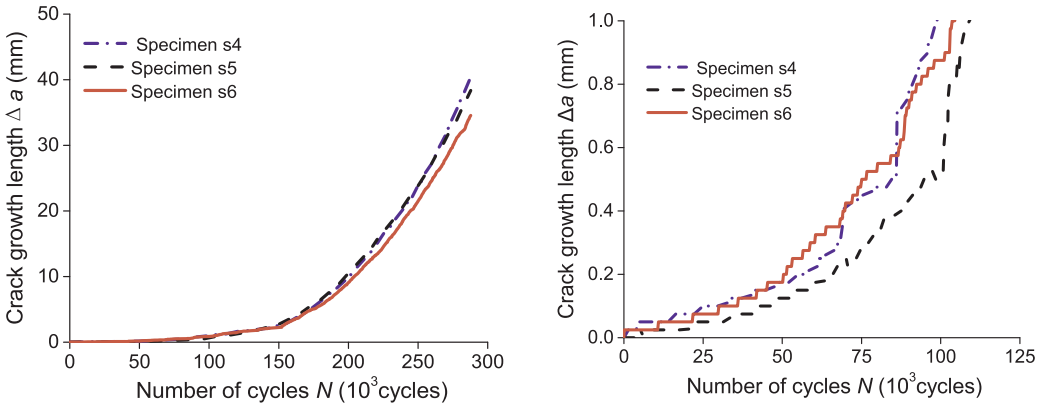

(a) The whole process of crack growth. (b) The local process of crack growth.

Fig. 9. The experimental crack growth length with the increase of number of cycles.

The modeling of rubber crack propagation behavior

The crack propagation rule based on the conventional secant and seven-point polynomial methods

The secant method and the seven-point polynomial method are two conventional methods to deal with the crack length to obtain the corresponding crack propagation rate. The secant method to get the crack propagation rate is expressed as [10]:

$$\left(\frac{da}{dN}\right)_i \approx \frac{a_{i+1}-a_i}{N_{i+1}-N_i} \tag{6}$$

where the subscript i is one positive integral and its maximum is up to the number n of data points minus 1, namely $n-1$; a_i represents the crack length at the number of cycles N_i.

The seven-point polynomial method (also called incremental polynomial) is to select successive seven points from the mass data of crack length a versus number of cycles N, and approach these seven points with one quadratic polynomial to get the local fitting formula, which differentiates the number of cycles to obtain the crack propagation rate. The crack propagation rate with the seven-point polynomial method is obtained as [10]:

$$\left(\frac{da}{dN}\right)_{N_i} = \frac{b_1}{C_2} + \frac{2b_2(N_i-C_1)}{C_2^2} \tag{7}$$

where the subscript i is the sequence number apart from the previous three and last three points of the measured data points; b_1 and b_2 are the regression coefficients based on the least square method. C_1 and C_2 are determined from the following equations:

$$C_1 = 1/2(N_{i-3} + N_{i+3})$$
$$C_2 = 1/2(N_{i+3}-N_{i-3}) \tag{8}$$

Taking specimen s4 for example, the crack propagation rate is obtained using the conventional secant and seven-point polynomial methods from the data of measured crack length and the number of cycles, which is shown in Figs. 10 and 11 with the corresponding maximum tearing energy as the abscissa, respectively. As shown in Figs. 10 and 11, the data of the crack propagation rate based on the secant method and the seven-point polynomial method is highly dispersed. It can be seen from Figs. 10 and 11 that the crack propagation rate is negative when the maximum tear energy is smaller than 1200 J/m2 and the crack propagation rate is always positive when the maximum tearing energy becomes larger than 1200 J/m^2. Similar results are found for specimens s5 and s6. The negative crack propagation rate with the increase of the maximum tearing energy is beyond understanding, and the frequently reported power law is not appropriate for unifying the relationship between the crack propagation rate and the maximum tearing energy. Therefore, an alternative data processing method for obtaining the crack propagation rate based the measured crack length and the number of cycles under variable amplitude loading instead of constant amplitude loading should be considered.

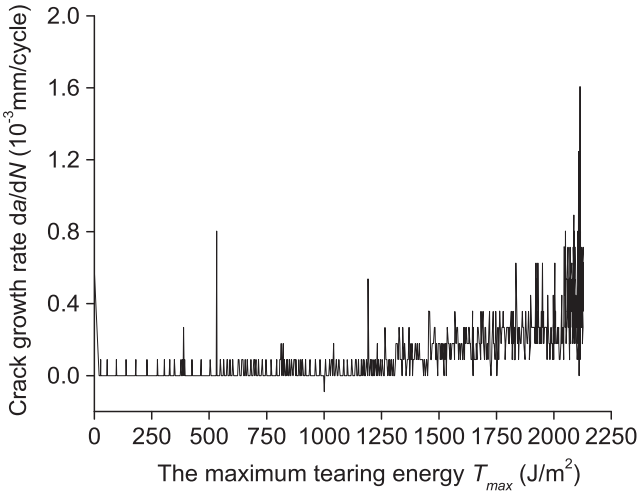

Fig. 10. The relationship between crack growth rate and the number of cycles using the secant method (Specimen s4).

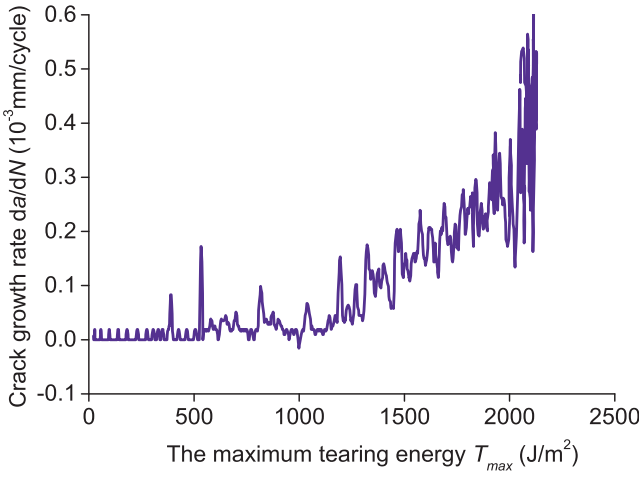

Fig. 11. The relationship between crack growth rate and the number of cycles using the seven-point polynomial method (Specimen s4).

The interpolation method with one power function

According to the shortcomings of the two methods above, one interpolation method with the power function is proposed to deal with the measured crack propagation data under variable amplitude loading, and then the model for characterizing the crack propagation length and the number of cycles is obtained.

It can be seen from Eq. (3) that the crack propagation rate of rubbery materials satisfies the relation of power function. It can be seen from Eq. (4) that the tearing energy of pure shear specimens is proportional to strain energy density. It can be seen from Fig. 7 that the relation between the maximum strain and the number of cycle are linear. Based on the mentioned information and the observation of Fig. 9, it can be assumed that the crack propagation length and number of cycles of pure shear specimens are approximately satisfying the relation of one power function.

When using a power function to globally approximate the data of crack propagation length and number of cycles, the effective data source should be firstly selected from the original measured data. It can be seen from Fig. 9b that the crack propagation rate in the early stage experiences one region that is fast to slow and rapidly growing. This is because the sharp crack has larger crack propagation rate than a natural rough crack. The initial crack given by the blade is sharp enough, and the stress concentration of the crack tip is higher. The sharp crack has a larger effective tear energy than the natural rough crack, and the difference between the two crack propagation rules has been studied in the literature [3]. Therefore, the load cycles initially applied in the test is considered to be used to pre-cycle the prefabricated sharp cracks to form a natural rough crack. The crack propagation path from Fig. 12 also shows that the sharp crack grows to form the natural rough crack at the beginning of the loading cycles. It can be found from Fig. 12 that crack tip slightly change in the early stage, but after a certain load cycles the crack tip keep expanding in vertical to the direction of imposed loads.

The data of crack propagation length Δa after 1 mm and the corresponding number of cycles (N) as the effective data source to establish the global relationship for characterizing the crack propagation length and the number of cycles. Based on the nonlinear least square method, the relationship between the crack propagation length (Δa) and the number of cycles (N) of the pure shear specimen is obtained using the power function as follows.

$$\text{Specimen s4:}\quad \Delta a = 1.42855 \times 10^{-20}(N_f)^{3.92965}, \quad r^2 = 0.9905 \tag{9}$$

$$\text{Specimen s5:}\quad \Delta a = 4.31014 \times 10^{-21}(N_f)^{4.02823}, \quad r^2 = 0.9970 \tag{10}$$

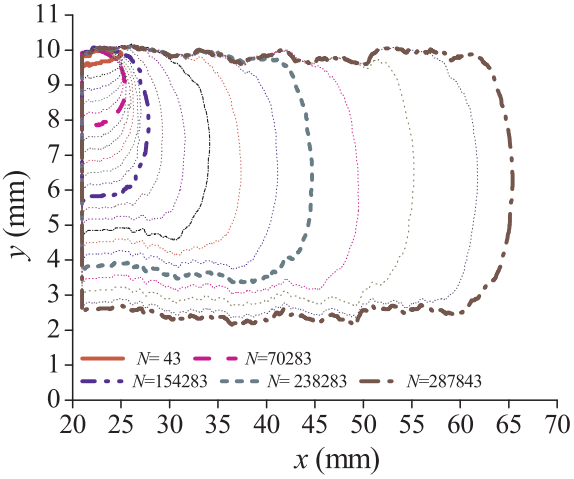

Fig. 12. Crack tip evolution with the increase of number of cycles (Specimen s4).

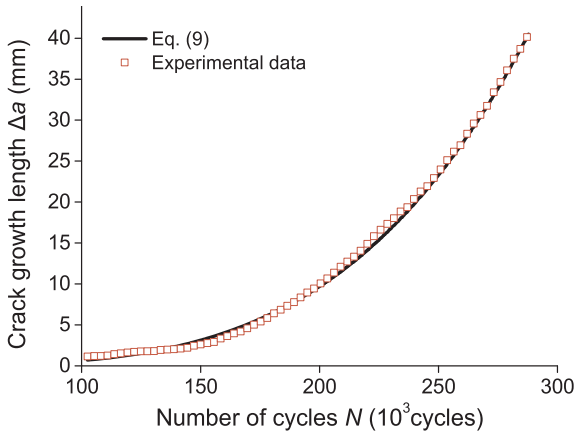

Fig. 13. The relationship between crack growth rate and the number of cycles using the interpolation method with one power function (Specimen s4).

$$\text{Specimen s6:}\quad \Delta a = 9.61766 \times 10^{-20}(N_f)^{3.76660}, \quad r^2 = 0.9891 \tag{11}$$

where the correlation coefficient of the fitting of the power function is larger than 0.99, which means that the fitting precision is high enough.

Taking specimen s4 for example, a comparison of the calculated crack propagation length from Eq. (9) and the measured result is shown in Fig. 13, which shows a high correlation. It should be noted that the effective numbers of parameters in the upper formula has a great influence on the calculation results since the magnitude of the number of cycles N is much larger than the length of crack propagation. It is found from the experiment that the proposed model parameters must be kept at least four decimal places to avoid the influence of data truncation error. Therefore, the parameters in the upper formula have values with 5 decimal places, and finally the parameters in the crack propagation rate model keep 4 decimal places to minimize data truncation error affecting the results.

Establishment of fatigue crack propagation rate model

In order to get the relationship between the crack propagation rate and the maximum tearing energy, Eqs. (9)–(11) should firstly differentiate with respect to the number of cycles N, to obtain the crack propagation rate of specimens s4–s6, respectively. The values of calculated crack propagation rate based on Eqs. (9)–(11) and the corresponding maximum tearing energy in Fig. 8 are then plotted in Fig. 14. It can be seen that the fluctuation of crack propagation rate is very small and the crack propagation rule is more consistent with the power

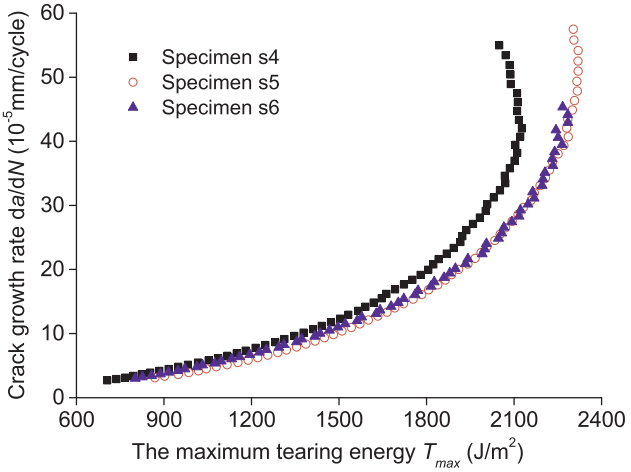

Fig. 14. The relationship between crack growth rate and the maximum tearing energy.

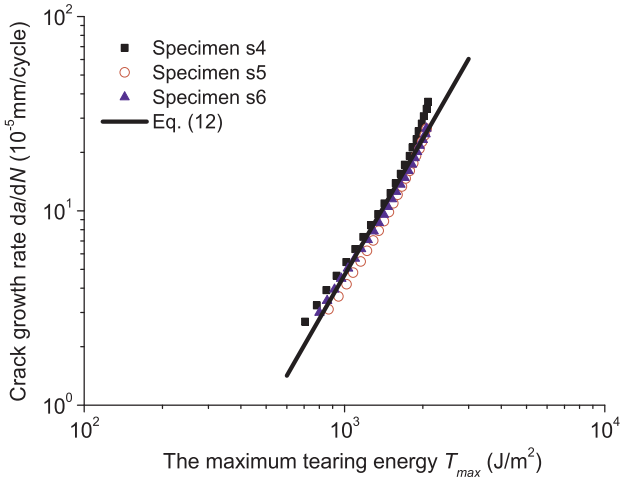

Fig. 15. The comparison between the fitted curve and the measured data for specimens s4–s6 (in log-log coordinate).

law when using the interpolation method of power function (Fig. 14), compared to the secant method (Fig. 10) and the seven-point polynomial method (Fig. 11).

It can be seen from Fig. 14 that the crack propagation rate of the three specimens increases rapidly when the maximum tearing energy is larger than 2100 J/m^2. The reason for the remarkable acceleration of crack propagation rate is the result of temperature accumulation effects at the end of the experiment, and the crack propagation mechanism in the region is more complex. Therefore, the data in the region of $T_{\max} < 2100$ J/m^2 in Fig. 14 are taken to determine the power relationship of crack propagation rate and the maximum tearing energy.

The crack propagation rate model is obtained by approaching the data of the three specimens in Fig. 14 based on nonlinear least square method as:

$$\mathrm{d}a/\mathrm{d}N = AT_{\max}^{F} = 4.65802 \times 10^{-12}(T_{\max})^{2.33362} \tag{12}$$

The correlation coefficient is $r^2 = 0.9678$. The comparison between the fitting curve and the measured data in the double-log coordinate is shown in Fig. 15, which shows that the fitting formula (12) is in good agreement with the measured data.

The critical crack propagation rate can be determined as follows:

$$r_c = AT_c^F = 3.66499 \times 10^{-5}\ (\mathrm{m/cycle}) \tag{13}$$

The equivalent crack propagation rate model of formula (12) with substituting Eq. (13) into Eq. (3) is expressed as:

$$\mathrm{d}a/\mathrm{d}N = r_c(T_{\max}/T_c)^F = 3.6650 \times 10^{-5}(T_{\max}/17400.7)^{2.3336}\ (\mathrm{m/cycle}) \tag{14}$$

Application examples

In order to apply the established fatigue crack propagation rate model, fatigue lives of dumbbell specimens (shown in Fig. 3) are calculated through integrating the established crack propagation rate model shown in Eq. (14), and then compared with the measured lives. The uniaxial tensile fatigue tests of identical rubbery materials were conducted on dumbbell specimens.

The tearing energy of the edge-notched simple tensile specimen such as dumbbell specimens (shown in Fig. 3) can be calculated using the following expression [3]:

$$T = 2kWa \tag{15}$$

where W is the strain energy density of far-field away from the crack; a is the crack length; K is a coefficient related to the strain level of materials and the tip of the crack tip [3]:

$$k = \frac{2.95-0.08\varepsilon_{\max}}{(1+\varepsilon_{\max})^{1/2}} \tag{16}$$

The calculation formula of fatigue life of rubbery materials under uniaxial fatigue tensile load can be calculated by substituting Eq. (15) into Eq. (14) and taking integration of Eq. (14), which is expressed as:

$$N_f = \frac{1}{F-1}\frac{r_c^{-1}T_c^F}{(2kW)^F}(a_0^{1-F}-a_f^{1-F}) \tag{17}$$

where a_0 represents the initial crack size of the blank material; a_f represents the maximum crack size which corresponds to fatigue fracture of the material. When the tearing energy reach the critical tearing energy (T_c), the material gets fatigue fracture. Therefore, the maximum crack size can be solved by letting the tearing energy in Eq. (15) equal to the critical tearing energy T_c as:

$$a_f = T_c/2kW \tag{18}$$

Substituting Eq. (18) into Eq. (17) can be obtained:

$$N_f = \frac{1}{F-1}\frac{r_c^{-1}T_c^F}{(2kW)^F}\left[a_0^{1-F}-\left(\frac{T_c}{2kW}\right)^{1-F}\right] \tag{19}$$

where kW could be determined once given the applied fatigue load on specimens.

In order to calculate the fatigue life using Eq. (19), the initial crack size a_0 should be given. The original defect size of rubbery materials is generally distributed between 2.0×10^{-5} m$\sim 6.0 \times 10^{-5}$ m [15]. The uniaxial tensile fatigue lives of rubbery materials under three different initial crack sizes (namely the initial crack size is given as 60 μm, 40 μm and 20 μm, respectively) are calculated from Eq. (19), noted as N_{p1}, N_{p2} and N_{p3} listed in Table 3, respectively.

The fatigue tests of dumbbell specimens is referred to Ref. [2]. In the fatigue tests, ten different loading cases of strain peak (the maximum strain per cycle) were performed and 20 identical rubber dumbbell specimens were tested in each loading case. The measured average lives

Table 3
Comparisons between the calculated lives and the measured lives with different initial crack sizes.

Load case	Strain peak $\varepsilon_{\max}$	Strain valley $\varepsilon_{\min}$	Calculated life N_p (cycle)			Measured average fatigue life N_m (cycle)	The ratio of calculated life and measured life		
			N_{p1}	N_{p2}	N_{p3}		N_{p1}/N_m	N_{p2}/N_m	N_{p3}/N_m
1	1.83	0.00	15,617	26,869	67,827	25,181	0.62	**1.07**	2.69
2	1.61	0.00	22,097	38,006	95,910	38,967	0.57	**0.98**	2.46
3	1.35	0.00	35,977	61,854	156,044	62,206	0.58	**0.99**	2.51
4	1.23	0.00	46,766	80,390	202,780	82,049	0.57	**0.98**	2.47
5	1.19	0.00	51,371	88,301	222,725	100,290	0.51	**0.88**	2.22
6	1.00	0.00	84,751	145,644	367,289	139,460	0.61	**1.04**	2.63
7	0.93	0.00	104,770	180,032	453,977	185,560	0.56	**0.97**	2.45
8	0.82	0.00	152,008	261,171	658,515	312,590	0.49	**0.84**	2.11
9	0.71	0.00	234,248	402,425	1,014,577	398,730	0.59	**1.01**	2.54
10	0.62	0.00	354,082	608,242	1,533,366	522,450	0.68	**1.16**	2.93

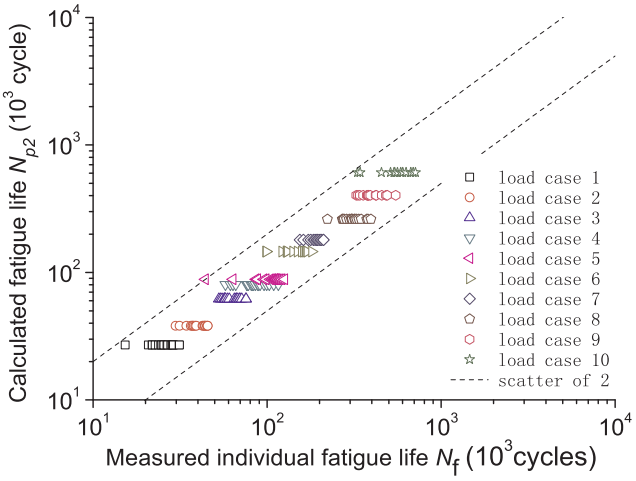

Fig. 16. The comparison between the measured life and the calculated life with the crack growth rate model.

obtained by averaging 20 measured lives in each loading case are shown in Table 3.

It can be seen from Table 3 that the initial crack size has great influence on the calculation results. The calculated results of fatigue life are best consistent with the measured results when the initial crack size $a_0 = 4.0 \times 10^{-5}$ m, shown in Fig. 16. According to Table 3 and Fig. 16, the prediction lives based on the crack propagation rate model shown in Eq. (14) fall within two times of the measured lives, which demonstrates a high accuracy of the crack propagation rate model established above.

Conclusions

(1) Using variable amplitude loading is more effective than constant amplitude loading in fatigue crack propagation experiments of rubbery materials. However, an alternative data processing method to determine the crack propagation rate based on the measured dispersed data should be considered. The proposed interpolation method of one power function to approach the measured crack propagation length and number of cycles shows a reasonable and convenient way.

(2) The established fatigue crack propagation rate model based on the power law is applied to predict the uniaxial fatigue life of rubbery materials. Once given the appropriate initial flaw size, the predictive lives fall within two times of measured lives, which shows a high accuracy.

(3) Some key points should be taken into consideration using the proposed interpolation method including: 1) an effective data source should be selected from the original measured data through the analysis of the measured data of the crack propagation length and the number of cycles. The data that the crack propagation rate increases with the decrease of the tearing energy should be eliminated; 2) the effective numbers of parameters in the model has a great influence on the calculation results since the magnitude of the number of cycles N is much larger than the length of crack propagation. The proposed model parameters must be kept at least four decimal places to avoid the influence of data truncation error.

Acknowledgements

The authors gratefully acknowledge the financial support of the National Natural Science Foundation of China (grant numbers 51505091, 51705128), and Guangdong Natural Science Foundation (grant number 2014A030310125). The authors also thank Prof. W.B. Shangguan, the postgraduate students T.K. Liu, X. X Xie from South China University of Technology for their work in experiments in the present work.**Data availability**

The raw data required to reproduce these findings cannot be shared at this time due to legal or ethical reasons.

References

[1] LuTee Yun, Loo Mei Sze, Andriyana Andri. Recent advances on fatigue of rubber after the literature survey by Mars and Fatemi in 2002 and 2004. Int J Fatigue 2018;110:115–29.
[2] Wenbin Shangguan, Xiaoli Wang, Jianxiang Deng, et al. Experiment and modeling of uniaxial tension fatigue performances for filled natural rubbers. Mater Des 2014;58:65–73.
[3] Gent AN, Lindley PB, Thomas AG. Cut propagation and fatigue of rubbers. I. The relationship between cut propagation and fatigue. J Appl Polym Sci 1964;8:455–66.
[4] Yeoh OH. Analysis of deformation and fracture of pure shear rubber test piece. Plast Rubber Compos 2001;30(8):389–97.
[5] Mars WV, Fatemi A. Fatigue crack nucleation and propagation in filled natural rubber. Fatigue Fracture Eng Mater Struct 2003;26:779–89.
[6] Kaang SY, Jin YW, Huh YI, et al. A test method to measure fatigue crack propagation rate of rubbery materials. Polym Test 2006;25:347–52.
[7] Zhipin Ding, Jipin Chen, Chuanjian Song, et al. Analysis of fatigue crack growth life for rubber vibration damper. J Mech Eng 2010;46(22):58–64. [in Chinese].
[8] Fayong Jia, Lixing Huo, Yufeng Zhang, et al. Comparison with two data processing methods on fatigue crack growth rate. J Mech Strength 2003;25(5):568–71. [in Chinese].
[9] Xianhong Meng, Xing Zhang. Method of integration in determination of the fatigue crack growth rate. J Mech Strength 2001;23(2):213–5. [in Chinese].
[10] American Society of Mechanical Engineers. ASME E 647–08 Standard test method for measurement of fatigue crack propagation rates. West Conshohocken: ASME; 2008.
[11] Zehnder Alan T. Lecture notes on fracture mechanics. New York: Cornell University Press; 2008.
[12] Griffith AA. The phenomena of rupture and flow in solids. Philos Trans R Soc London, Ser A, Containing Papers of a Mathematical or Physical Character 1921;221:163–98.
[13] Thomas AG. Rupture of rubber. V. Cut propagation in natural rubber vulcanizates. J Polym Sci 1958;31:467–80.
[14] Lindley PB. Relation between hysteresis and the dynamic crack propagation resistance of natural rubber. Int J Fract 1973;9(4):449–62.
[15] Lake GJ. Fatigue and fracture of elstomers. Rubber Chem Technol 1995;68(3):435–59.
[16] Mars WV, Fatemi A. A phenomenological model for the effect of R ratio on fatigue of strain crystallizating rubber. Rubber Chem Technol 2003;76:1241–58.
[17] American Society of Mechanical Engineers. ASTM Standard D4482-99 Standard test method for rubber property-extension cycling fatigue. West Conshohocken: ASME; 1999.